THE ASTROPHYSICAL JOURNAL, 543:216–226, 2000 November 1
© 2000. The American Astronomical Society. All rights reserved. Printed in U.S.A.

COOLING SEQUENCES AND COLOR-MAGNITUDE DIAGRAMS FOR COOL WHITE DWARFS WITH HYDROGEN ATMOSPHERES

G. CHABRIER,[1] P. BRASSARD,[2] G. FONTAINE,[2] AND D. SAUMON[3]

Received 2000 March 4; accepted 2000 June 9

ABSTRACT

We present new cooling sequences, color-magnitude diagrams, and color-color diagrams for cool white dwarfs with pure hydrogen atmospheres down to an effective temperature $T_{\rm eff} = 1500$ K. We include a more detailed treatment of the physics of the fully ionized interior, particularly an improved discussion of the thermodynamics of the temperature-dependent ion-ion and ion-electron contributions of the quantum, relativistic electron-ion plasma. The present calculations also incorporate accurate boundary conditions between the degenerate core and the outermost layers as well as updated atmosphere models including the H_2-H_2 induced-dipole absorption. We examine the differences on the cooling time of the star arising from uncertainties in the initial carbon-oxygen profile and the core-envelope L-T_c relation. The maximum time delay due to crystallization-induced chemical fractionation remains substantial, from $\sim$1.0 Gyr for 0.5 and 1.2 $M_\odot$ white dwarfs to $\sim$1.5 Gyr for 0.6–0.8 $M_\odot$ white dwarfs, even with initial stratified composition profiles, and cannot be ignored in detailed white dwarf cooling calculations. These cooling sequences provide theoretical support to search for or identify old disk or halo hydrogen-rich white dwarfs by characterizing their mass and age from their observational signatures.

Subject headings: equation of state — Galaxy: halo — stars: atmospheres — white dwarfs

1. INTRODUCTION

The possible interpretation of the faint blue objects in the Hubble Deep Field (HDF) as halo white dwarfs (Hansen 1998; Ibata et al. 1999; Méndez & Minniti 2000), consistent with the interpretation of the observed microlensing events toward the Large Magellanic Clouds as stellar remnants (Chabrier, Segretain, & Méra 1996; Adams & Laughlin 1996; Graff, Laughlin, & Freese 1998; Chabrier 1999), and the spectroscopic identification of very cool ($T_{\rm eff} \lesssim 4000$ K), high proper motion white dwarfs (WDs) (Hodgkin et al. 2000; Ibata et al. 2000) have triggered interest in the study of old, cool WDs and stressed the need for accurate cooling sequences and predicted observational signatures for these objects. This implies a correct cooling theory for crystallized white dwarfs and reliable atmosphere models and photometric predictions.

The basic physics entering WD evolution has evolved significantly since the pioneering work of Mestel & Ruderman (1967) and the first detailed evolutionary calculations by Lamb & Van Horn (1975). Noteworthy advances have been made on the fronts of the conductive opacity (Itoh et al. 1983; Itoh, Hatashi, & Kohyama 1993; Potekhin et al. 1999), the radiative opacity (Lenzuni, Chernoff, & Salpeter 1991; Rogers & Iglesias 1992), the envelope equation of state (EOS) (Saumon, Chabrier, & Van Horn 1995, hereafter SCV95), and the detailed description of the thermodynamic properties of the dense, fully ionized interior plasma, including the main effects of ion crystallization, namely, the latent heat and the chemical fractionation (Segretain et al. 1994 and references therein). In the meantime, substantial improvement in the theory of the atmosphere of cool WDs has been accomplished (Bergeron, Wesemael, & Fontaine 1991; Bergeron, Saumon, & Wesemael 1995a, hereafter BSW95; Bergeron, Wesemael, & Beauchamp 1995b, hereafter BWB95).

These studies were devoted primarily to the characterization of the disk WD population and were thus restricted to effective temperatures $T_{\rm eff} > 4000$ K. As identified initially in BSW95, the onset of molecular recombination below $\sim$5000 K and the pending collision-induced absorption (CIA) due to H_2-H_2 and H_2-He collisions in such dense atmospheres ($g \simeq 10^8$–10^9 cm s^{-2}) result in important departures from a blackbody energy distribution, with an increasing absorption of the flux longward of 1 μm. The WD atmosphere calculations were extended recently to lower temperatures by Hansen (1998, 1999) and by Saumon & Jacobson (1999, hereafter SJ99), reaching the effective temperature range characteristic of the halo or globular cluster old WD population. As shown by these authors, the strong CIA in the infrared redistributes the flux toward shorter wavelengths so that the emergent flux peaks in optical passbands, regardless of $T_{\rm eff}$. This effect has been confirmed recently with the spectroscopic observation of H_2 CIA in LHS 1126 (Bergeron, Ruiz, & Leggett 1997), LHS 3250 (Harris et al. 1999), and WD 0346+246 (Hodgkin et al. 2000). As demonstrated initially by Hansen (1998), the colors of very cool WDs are consistent with the unidentified faint blue objects in the HDF (Bahcall et al. 1994; Méndez et al. 1996; Nelson, Santiago, & Gilmore 1996; Ibata et al. 1999). A preliminary set of cooling sequences incorporating the SJ99 synthetic colors for cool WDs with pure H atmospheres provides luminosity and discovery functions in various passbands for a dark halo WD population consistent with the microlensing experiments (Chabrier 1999).

Current cooling models (Wood 1995; Segretain et al. 1994; Salaris et al. 1997; Montgomery et al. 1999) appear to be reasonably consistent with each other for WDs with

[1] Ecole Normale Supérieure de Lyon (C.R.A.L; UMR 5574 CNRS), 69364 Lyon Cedex 07, France.

[2] Département de Physique, Université de Montréal, C.P. 6128 Succ. A., Montréal, Québec, Canada H3C 3J7.

[3] Department of Physics and Astronomy, Vanderbilt University, P.O. Box 1807, Station B, Nashville, TN 37235.

$T_{\rm eff} \gtrsim 4000$ K, i.e., younger than ~ 10 Gyr for a 0.6 $M_\odot$ WD. For these temperatures, hydrogen molecular recombination is absent or negligible and the spectral energy distribution is moderately affected by H_2-H_2 or H_2-He CIA (see, e.g., BSW95). The aim of the present paper is to extend cooling calculations to older WDs that are characteristic of the disk, spheroid, or dark halo population. To this end, we use upgraded interior physics, synthetic spectra, and interior-envelope relations. A description of the various physical inputs entering the calculations and a comparison with previous calculations are given in § 2. Cooling sequences and color-magnitude and color-color diagrams in various optical and infrared passbands are presented in § 3, and the remaining uncertainties in the models are examined. Conclusions are presented in § 4.

2. MODEL CALCULATIONS

In the present paper we will concentrate on the so-called DA WDs, i.e., those having either pure hydrogen atmospheres or atmospheres with a small admixture of helium [N(He)/N(H) $\ll 1$]. The main reason is the fact that detectable halo WDs will very likely have hydrogen-rich atmospheres. It is indeed well known that white dwarfs with pure helium outer layers must evolve more rapidly than their DA counterparts at the faint end of the cooling sequence because of the extreme transparency of these layers. Explicit calculations, assuming such pure helium envelopes, show that He atmosphere halo WDs, if they exist, would escape detection since they reach $M_{\rm bol} \gtrsim 19$ after ~ 8 Gyr (Chabrier 1997; Hansen 1998). We note, however, that even very small traces of hydrogen or metals in their envelopes (possibly due to accretion, microscopic diffusion, or convective dredge-up) could change this picture dramatically. Indeed, such traces increase significantly the opacity of the otherwise transparent neutral helium at low effective temperatures, slowing down the cooling of the star. If hydrogen itself is present, even as a trace, the emergent spectrum is brought closer to that of a DA star.

Note also that reliable calculations of pure helium model atmospheres at very low effective temperatures remain to be done. For instance, accurate treatments of helium pressure ionization, as raised initially by Böhm et al. (1977; see also BSW95; Hansen 1998), and of He^- free-free absorption cross section at high densities are still lacking. While realistic model atmospheres of non-DA WDs are available for $T_{\rm eff} > 4000$ K (BSW95; BWB95) and reasonable estimates of their cooling timescales have been published (Wood 1995; Segretain et al. 1994; Salaris et al. 1997), the same cannot be said for the cooler end of the sequence. Fortunately, as mentioned above, the most probable cases of detection of halo WDs are identified with DA stars.

2.1. *Core Physics*

2.1.1. *Equation of State*

In the present paper we consider only WDs with carbon-oxygen cores, which restricts the mass range to $0.5 \leq M \leq 1.2\ M_\odot$. We define the core as the region where the C/O plasma is fully ionized and the electron gas is fully degenerate. The large electron conductivity ensures that the core is very nearly isothermal. This essentially isothermal domain encompasses typically 99.99% of the mass of cool WDs (see, e.g., Fig. 14 of Tassoul, Fontaine, & Winget 1990). In this region we adopt the equation of state (EOS) described in § 2 of Segretain et al. (1994) for the liquid and solid phases:

$$U_L(x_i, \rho, T) = U_i^{\rm id} + U_i^{\rm ex} + U_e^{\rm id} + U_e^x + U_{\rm ie}\ , \quad (1)$$

$$U_S(x_i, \rho, T) = U_i^{\rm th} + U_i^{\rm anh} + U_i^{\rm qm} + U_i^{\rm Mad} + U_e^{\rm id} + U_e^x + U_{\rm ie}\ , \quad (2)$$

where the different contributions are described in Segretain et al. (1994) ($x_i = N_i/N$ denotes the number fraction of each element, C and O).

In the present calculations, we introduce a major improvement with respect to Segretain et al. (1994) that is essential for cool, crystallized WDs. In Segretain et al. (1994) and in further calculations based on this EOS, the ion-electron screening contribution, $U_{\rm ie}$, was taken from Yakovlev & Shalybkov (1989, hereafter YS89). As stressed by these authors, their calculations are valid only in the fluid phase, where the plasma ion coupling parameter $\Gamma = 2.275 \times 10^5 \langle Z^{5/3}\rangle [(\rho Y_e)^{1/3}/T] \lesssim 200$, where $Y_e = \langle Z\rangle/\langle A\rangle$ is the average electron molar fraction and $\langle Z^{5/3}\rangle = \sum_i x_i Z_i^{5/3}$. The arrow in Figure 1 indicates the luminosity at which the ion coupling parameter at the center of the star reaches the aforementioned value 200 for a 0.6 $M_\odot$ WD. As shown in the figure, extrapolation of the YS89 fit in the solid phase ($\Gamma > 200$) yields an increasingly inaccurate cooling sequence. Note also that the YS89 fit is derived from calculations of the thermodynamic properties of a classical ionic plasma, whereas the C/O solid core is in a quantum state, with an ion diffraction parameter $\hbar\Omega_P/kT > 1$, where Ω_P denotes the ion plasma frequency (see Segretain et al. 1994). The Segretain et al. (1994) study was primarily devoted to disk WDs, i.e., objects brighter than $\log (L/L_\odot) \sim -4.5$. This corresponds approximately to the end of the crystallization process in WD interiors. Halo WDs, however, are fainter than $10^{-4.5}\ L_\odot$ and $\Gamma > 200$ throughout a large fraction of the star.

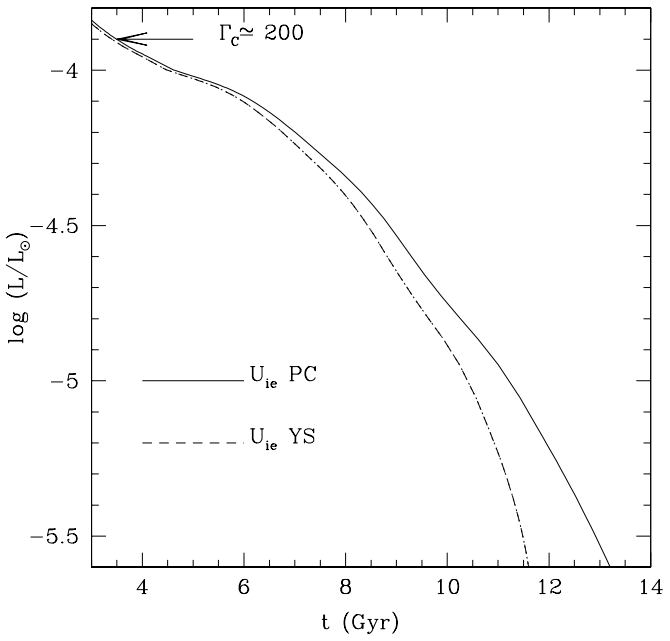


FIG. 1.—Cooling sequence for a 0.6 $M_\odot$ WD with the ion-electron contribution in the solid calculated by Potekhin & Chabrier (2000) (*solid line*) or extrapolated from Yakovlev & Shalybkov (1989) (*dashed line*). The arrow indicates the value $\Gamma_c = 200$ for the plasma parameter at the center of the star.

In fully crystallized WDs, there is no further contribution to the luminosity from crystallization-induced chemical fractionation of C and O (see Segretain et al. 1994; Chabrier 1997; Isern et al. 1997). The only contributions to the luminosity come from the thermal reservoir of the star and from the residual gravitational contraction of the outermost layers (see, e.g., Koester & Chanmugam 1990; D'Antona & Mazzitelli 1990):

$$\frac{dL}{dt} = -\int_0^M C_V \frac{dT}{dt} dm - \int_0^M \left(T \frac{dP}{dT} \right) \frac{dv}{dt} dm . \quad (3)$$

Note that the thermal energy (first term on the right-hand side of eq. [3]) is comparable to the change in gravitational energy $\Delta\Omega$, from the virial theorem. For a substantially (entirely) crystallized WD, most of (all) the thermal energy stems from the specific heat of the quantum solid. Although for very cool WDs the thermal contribution of the central regions, where $\hbar\Omega_P/kT \gg 1$, becomes increasingly small, the contribution of the outer layers, where $\hbar\Omega_P/kT \sim 1$, remains substantial. Indeed, in cool WDs, the main contributions to the internal energy, namely, the zero-temperature electron gas kinetic energy $U_e^{\rm id}$ and the ionic electrostatic energy $U_i^{\rm Mad}$ in equation (2) (see Fig. 1 of Segretain et al. 1994), do not depend on temperature, so that the heat capacity, and thus the cooling, is entirely determined by the small temperature-dependent *corrections* to the energy. In fact, the ion-electron screening contribution, which stems from the polarization of the electrons by the ionic field, becomes the *dominant* contribution to the specific heat at low temperature since it decreases as $C_{V_{\rm ie}} \propto \eta^{-1} \propto T$, whereas the ionic crystal (Debye) contribution decreases as $C_{V_{\rm ii}} \propto \eta^{-3} \propto T^3$ (Potekhin & Chabrier 2000).

For fully crystallized WDs, the central density is of the order of $\rho_c \simeq 10^6$ g cm^{-3}, so that the Fermi parameter $x = p_{\rm F}/m_e c = 1.01 \times 10^{-2} (\rho Y_e)^{1/3} > 1$. Therefore, we must consider the energetic contribution due to the ion-electron interaction of a polarizable, relativistic electron gas immersed in a quantum Coulomb crystal. The Thomas-Fermi approximation (Salpeter 1961) is valid only in the asymptotic limit of an infinite ionic charge $Z \rightarrow \infty$ and is not valid for a C^{6+}/O^{8+} plasma (see, e.g., YS89). The ion-ion and ion-electron contributions to the EOS of a quantum electron-ion solid plasma for a finite ionic charge under the conditions of interest have been calculated recently by Potekhin & Chabrier (2000). To the best of our knowledge these are the only available calculations for such plasma conditions. Figure 1 compares the evolution of a 0.6 $M_\odot$ crystallized WD for the same $T_{\rm eff}$-T_c condition (as described below) with the solid EOS and specific heat incorporating (1) the proper ion-electron screening treatment and (2) an extrapolation of the YS89 fit. As shown, the extrapolation yields increasingly shorter cooling times for WDs older than ~ 8 Gyr.

The contribution of crystallization along evolution is treated as described in § 4 of Segretain et al. (1994), from the evolution of the binding energy, $dB(T)/dt$. Recent complete evolutionary calculations by Montgomery et al. (1999) confirm the validity of this method for cool WDs, where there is no neutrino or nuclear luminosity. The crystallization of ^{22}Ne, which yields an azeotropic diagram (Segretain & Chabrier 1993) and was originally thought to produce a significant time delay (Isern et al 1991; Segretain et al. 1994), has not been considered in the present calculations. Indeed, consistent calculations of the three-body Ne/C/O phase diagram (Segretain 1996) show that when Ne crystallization sets in, a substantial fraction of oxygen has already crystallized, yielding an O-rich core, so that the remaining amount of energy due to ^{22}Ne crystallization becomes fairly small. At the crystallization luminosity found in Segretain et al. (1994), the induced time delay is at most ~ 0.3 Gyr, well within the remaining uncertainties in our calculations (phase diagram, opacities, etc.). In any event, since we are presently interested mainly in old WDs originating from low-metallicity progenitors, the Ne abundance is likely to be too small to have any measurable effect.

2.1.2. *Initial Carbon-Oxygen Profiles*

Substantial uncertainty remains on the ^{12}C(α, γ)^{16}O reaction that determines the final state of the He-burning asymptotic giant branch (AGB) phase and thus the initial C/O abundance profile of the WD. Modern experimental data and updated values of the astrophysical S-factor (see, e.g., Arnould et al. 1999) suggest a rate about a factor of 1.5–2 larger than that of Caughlan & Fowler (1988, hereafter CF88), closer to the previous Caughlan et al. (1985) value. This yields a substantially O-enriched initial profile in the WD core (see, e.g., Salaris et al. 1997). We have adopted these initial profiles in our calculations. However, in order to examine the uncertainties due to the interior composition, we have also conducted calculations for a 0.6 $M_\odot$ WD with an initial C/O distribution resulting from the CF88 lower rate (see Fig. 2 of Salaris et al. 1997).

2.2. *The Luminosity–Central Temperature Relation*

The binding energy method that we use to compute cooling ages relies on the availability of L-T_c relations, which govern the cooling rates of WDs. These relations are particularly sensitive to the constitutive physics of the outer partially ionized, partially degenerate envelope that connects the nearly isothermal core of a WD to its surface (the atmospheric layers). Previous calculations based on this method (Segretain et al. 1994 and references therein; Salaris et al. 1997) used L-T_c relations provided by independent model calculations such as, for example, those of Wood & Winget (1989) or Wood (1995). This approach necessarily introduces some inconsistencies in the calculations: the chemical composition of the core of the models used to derive the L-T_c relation differs from the variable core composition of the nearly isothermal structure that undergoes phase separation, and the constitutive physics is generally different in the two sets of models. Moreover, for masses not directly available from independent models, L-T_c relations were *scaled* on the mass, which, at best, provides a rough estimate of the correct relations.

We have improved on this front in the present paper by computing L-T_c relations based on state-of-the-art constitutive physics and by considering several individual masses. We are still left with the inherent inconsistency of the binding energy approach as a result of the fixed interior composition in the calculation of the L-T_c relation, but this shortcoming is largely offset by our ability to describe in accurate details the physics of crystallization (e.g., the phase diagram) or the radiative and conductive opacities at high density, or by the aforementioned uncertainties in the stratified C/O profile. Note also that the treatment of

crystallization-induced fragmentation can be easily implemented in the binding energy method, whereas it is a complicated task to include it in a standard evolutionary code. At this level, the binding energy method shows an appreciable advantage. Moreover, as mentioned above, the validity of this method for cool WDs has been assessed recently by comparisons with complete evolutionary calculations (Montgomery et al. 1999).

The L-T_c relations for various masses in the range of interest were computed with an upgraded version of the stellar model building code briefly described in Brassard & Fontaine (1994, 1997). These are *full* stellar models that describe the complete structure of a static WD from the center to the high atmosphere ($\tau_R \sim 10^{-6}$, where τ_R denotes the Rosseland optical depth). The envelope calculation incorporates the SCV95 EOS for H and He and the Fontaine, Graboske, & Van Horn (1977) EOS for carbon and oxygen. The radiative opacities include the OPAL 1996 data (Iglesias & Rogers 1996) complemented at low temperatures by the Rosseland opacities of H and He computed with the model atmosphere code of BSW95 down to 1500 K for H and 2500 K for He. These latter opacities include the complete CIA processes (see BSW95). For the conductive opacities, we use a large table incorporating the Hubbard & Lampe (1969) and Itoh et al. (1983, 1993) calculations (Brassard & Fontaine 1994), which covers the entire density and temperature range relevant to the present calculations. Convection is described with the standard mixing-length theory. As shown in Tassoul et al. (1990), the L-T_c relationship is insensitive to the assumed convective treatment, since convection is essentially adiabatic when it breaks through the degenerate core.

We note that Hansen (1998, 1999) has recently emphasized the importance of treating in detail the atmospheric layers in the context of the evolution of very cool WDs. As discussed initially by Fontaine & Van Horn (1976; see also Tassoul et al. 1990), the most important consequence of such a detailed description of the atmosphere on the cooling is its effect on the location of the base of the convection zone in the deeper, optically thick envelope. Indeed, below a luminosity $\log (L/L_\odot) \sim -3.7$ ($T_{\rm eff} \simeq 5500$–6500 K), the base of the hydrogen superficial convection zone reaches into the degenerate core, thus coupling, for the first time during the evolution, the atmospheric layers with the central thermal reservoir. Since, by then, the stratification of the envelope is fully convective and highly adiabatic, small changes at the base of the atmosphere produce corresponding changes at the base of the convection zone. A correct determination of the base of that zone is thus essential to calculate an accurate L-T_c relation for cool WDs.

It is important to stress that, although the atmospheric structures entering the present stellar models are gray, they take into account the feedback effect of convection on the atmospheric structure and thus are not based on a Rosseland mean all the way through, unlike those used in all previous evolutionary calculations, with the exception of Hansen's (1998, 1999) computations. These modified model atmospheres, to be described elsewhere (P. Brassard & G. Fontaine 2000, in preparation), reproduce almost exactly the stratification of a detailed model atmosphere (from, e.g., BSW95 in the present context) at large optical depths. They reproduce well, in particular, the main effect due to nongrayness, namely, the upward shift of the convection zone. This phenomenon is well known in stellar atmosphere theory and has been described, in a white dwarf context, by Böhm et al (1977) among others. Therefore, the boundary conditions provided by the detailed model atmosphere at $\tau_R = 100$ are essentially the same as those provided by the gray model with convective feedback. This is what matters for the cooling; for nearly identical boundary conditions at the base of the convective atmosphere, we find the same location of the base of the full envelope convection zone and hence the same value of T_c. In contrast, standard gray atmosphere stratification (not taking into account the feedback due to convection) leads to an incorrect determination of the base of the convective zone, overestimating its penetration and thus yielding a faster cooling (see § 3.1 below).

A central parameter in the envelope calculation and in the resulting cooling time is the amount of hydrogen and helium present in the envelope. For the present calculations, we have used DA white dwarf standard "thick" layers, $\log q({\rm H}) = -4.0$, $\log q({\rm He}) = -2.0$, where $q({\rm X}) = M({\rm X})/M_*$ denotes the mass fraction of element X. In practice, the masses of the hydrogen and helium layers on top of the degenerate C/O interior depend on the WD mass, through the AGB and post-AGB evolutionary phase (see, e.g., Blöcker et al. 1997). Note, however, that (1) calculations during the AGB phase strongly depend on ill-constrained parameters (overshooting, mass loss, etc.) and (2) present calculations consider the evolution of solar-metallicity AGB stars, whereas the progenitors of very cool WDs are metal depleted. Given these uncertainties in the exact amount of q(H) and q(He), we elected to conduct our calculations with the aforementioned "standard" values for a 0.6 $M_\odot$ WD (see Fontaine & Wesemael 1997 for a general discussion of this unsettled issue). This uncertainty in the exact amount of H and He in WD envelopes certainly represents one of the major uncertainties in present WD cooling calculations. Some scaling relations, however, can be used. Indeed, the effect of the thickness of the helium layer on the cooling time has been examined in detail by Tassoul et al. (1990), Wood (1992), and Montgomery et al. (1999, § 5.1). Thicker helium layers result in more transparent envelopes (since $\kappa_{\rm He} \ll \kappa_{\rm carbon}$ under WD conditions), decreasing the temperature gradient between the core and the surface, so that the central temperature decreases faster with decreasing luminosity. Therefore, models with thicker He layers are younger for a given mass and luminosity, with an $\sim$0.75 Gyr decrease in the age for each order of magnitude in $M_{\rm He}$ (Montgomery et al. 1999).

2.3. *Model Atmospheres and Photometric Colors*

The observable properties of the cooling WD, such as the emergent spectrum and the photometric colors, are obtained with atmosphere models. The present calculations include the colors and bolometric corrections for pure hydrogen atmospheres calculated by BSW95 above 4000 K, extended down to $T_{\rm eff} = 1500$ K by SJ99. As mentioned previously, for very cool WDs ($T_{\rm eff} \lesssim 5000$ K), molecular hydrogen becomes stable and the main source of opacity in the infrared is the CIA by H_2. This opacity forces the stellar flux to emerge at shorter wavelengths, with a peak near 1 μm. This increased flux in the R and I bands and decreased flux in infrared result in increasingly blue color indices for cooler WDs (Hansen 1998, 1999; SJ99).

Although similar to those done by Hansen (1998, 1999), the present calculations include a more detailed treatment of the microphysics entering the atmosphere (BSW95;

SJ99). Indeed, an important feature in these cool and dense atmospheres is the effect of the surrounding particles on the partition function of an atom, which eventually leads to the pressure ionization of hydrogen. These modified internal partition functions imply a different (nonideal) ionization equilibrium, in particular for the abundances of H_2, H_2^+, and H_3^+. This in turn modifies the abundance of free electrons, and thus of H^- ions, a dominant source of opacity in the optical. The atmosphere models of SJ99 were used in the range $1500 \leq T_{\rm eff} \leq 4000$ K and $7.5 \leq \log g \leq 9.0$, complemented by BSW95 for $4000 \leq T_{\rm eff} \leq 10{,}000$ K, with a pure hydrogen composition. These synthetic spectra and atmosphere models have been successfully confronted with available spectroscopic and photometric observations of cool H-rich (DA) WDs above 4000 K (Bergeron et al. 1997).

Optical colors for cool WDs with a small but nonzero N(He)/N(H) composition ratio will be only slightly different ($\lesssim$0.2 mag) from the colors of pure hydrogen atmospheres presented here (see BSW95; Bergeron et al. 1997). The color indices of Table 2 of BSW95 can then be used above 4000 K for mixed composition atmospheres.

3. RESULTS

3.1. *Cooling Curves*

For the purposes of comparisons, we define a set of reference models that include the physics described in the previous section, including crystallization-induced fragmentation (see below), with the Salaris et al. (1997) high-rate stratified initial C/O profiles. The L-T_c relations that we used for these reference models have been computed as described above, from full static stellar models with chemical layering defined by $\log q({\rm H}) = -4.0$ and $\log q({\rm He}) = -2.0$. The photometric colors are taken from pure H atmosphere calculations.

3.1.1. *Comparison with Existing Calculations*

We first compare, in Figure 2, our L-T_c relation for a 0.6 $M_\odot$ WD with the one obtained by Wood (1995), the one by Montgomery et al. (1999, Table 1), and another one kindly provided by Hansen (1999) for the same values of q(H) and q(He). The four curves agree reasonably well, but the relatively small differences shown here translate into significant differences on the cooling time (see below). Unfortunately, it is currently impossible to account in detail for the differences in the L-T_c relations illustrated in Figure 2; differences in the constitutive physics used by the various groups are probably at the origin of most of the deviations. The L-T_c relation is particularly sensitive to the opacity profile throughout the star, so slightly different implementations of the conductive and radiative opacities, as well as the use of different generations of these data, could very well account for most of the discrepancies. As expected, the Wood (1995) and the Montgomery et al. (1999) relations are very similar, since they rely on the same input physics, yielding similar cooling sequences.

As mentioned in § 2.2, the change of slope observed in all three curves is a well-known phenomenon and is due to convection breaking into the degenerate thermal reservoir at sufficiently low luminosities. When that occurs, there is a flattening of the temperature gradient between the core and the surface as a result of the larger efficiency of convection as compared to radiation. Initially, this leads to a slowdown of the cooling process as an excess energy is liberated through the more transparent convective envelope, but this

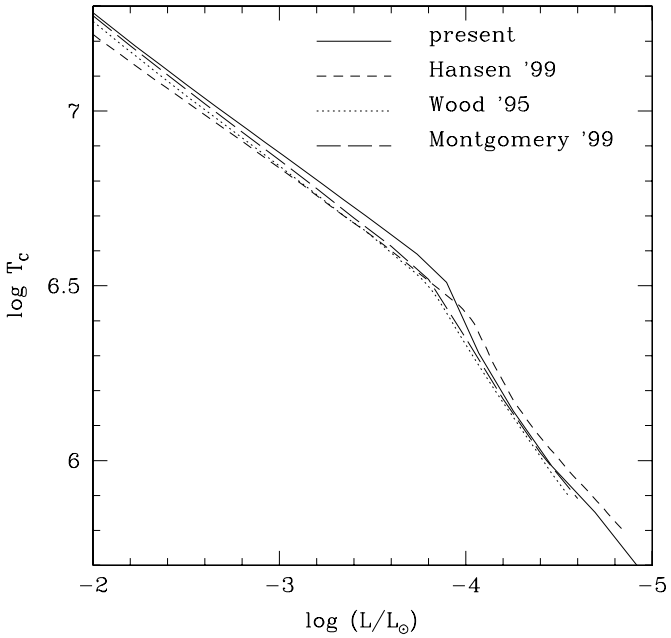


FIG. 2.—L-T_c relations from our calculations (*solid line*) and those of Hansen (1999) (*short-dashed line*), Wood (1995) (*dotted line*), and Montgomery et al. (1999) (*long-dashed line*) for a 0.6 $M_\odot$ WD with hydrogen and helium mass fractions $q({\rm H}) = 10^{-4}$, $q({\rm He}) = 10^{-2}$ and pure H atmosphere.

is rapidly followed by a phase whereby convection speeds up the cooling process as compared to the case of purely radiative models (see Fig. 3 of Tassoul et al. 1990 and related discussion). For luminosities lower than that of the breaks in slope shown in Figure 2, the L-T_c relation becomes sensitive, among other things, to the details of the atmosphere. From this point of view, the Hansen (1999) calculations and our own improve upon those of Wood (1995) or Montgomery et al. (1999) because the latter ones rely on a standard gray atmosphere strategy that overestimates the penetration of the superficial convection zone and leads to a value of T_c slightly lower than it should be, as discussed previously.

On the other hand, for luminosities larger than those of the changes of slope, it is well established that the relation is completely insensitive to the stratification of the upper envelope and, in particular, to the details of the atmosphere (see Tassoul et al. 1990 for a complete discussion). The discrepancies shown in Figure 2 between the three curves for these higher luminosities are then the explicit proof that there are indeed significant differences in the implementation/calculation of the constitutive physics between the three groups, notably at the level of the conductive opacities. So, to a certain extent, the differences found in Figure 2 result from the fact that we are comparing models with different physical inputs.

Figure 3 illustrates the consequences of these differences on the cooling time of the star. For each L-T_c relation, we show two cases: (1) taking into account the chemical fractionation of C and O at crystallization (*rightmost curves*) and (2) ignoring this process (*leftmost curves*). Interestingly enough, we find that in the phases of interest for the present study [$\log (L/L_\odot) < -4.5$], our results (*solid curves*) agree reasonably well with those obtained when using the L-T_c relation provided by Hansen (*long-dashed curves*). The results derived on the basis of the Wood (1995) (or Montgo-

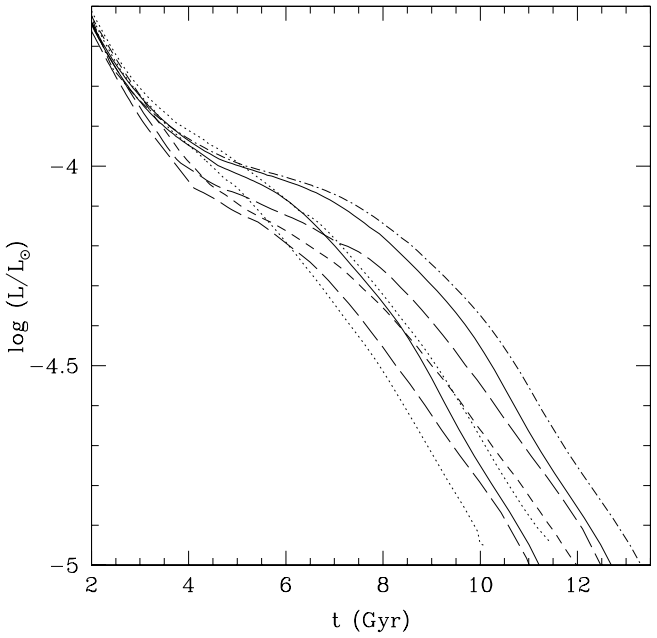


FIG. 3.—Cooling sequences with (*right curves*) and without (*left curves*) crystallization-induced fractionation for a 0.6 $M_\odot$ DA WD. *Solid curves*: calculations with our L-T_c relation; *long-dashed curves*: calculations with Hansen (1999) L-T_c relation; *dotted curves*: calculations with Wood (1995) L-T_c relation; *short-dashed curve*: Hansen (1999) cooling sequence; *dash-dotted curve*: present calculations with an initial profile obtained with a low $^{12}C(\alpha, \gamma)^{16}O$ reaction rate, with fractionation.

mery et al. 1999) L-T_c relation (*dotted curves*) provide, in comparison, shorter cooling timescales, as anticipated from the discussion above. The differences illustrated in Figure 3 simply amplify the differences already observed in the L-T_c relations of Figure 2.

Another interesting comparison is provided by the short-dashed curve in Figure 3, which presents the cooling curve obtained by Hansen (1999), which is supposed to include the complete treatment of crystallization and thus must be compared with the right long-dashed curve. The difference between the two curves is noticeable ($\gtrsim$0.5 Gyr) and cannot be totally ignored. Since such a comparison eliminates the effect of the energy transfer problem (the L-T_c relations are the same), the remaining discrepancies must be blamed mostly on the different treatments of the thermodynamics of the ionized interior, outlined in § 2.1.1. Since Hansen has not detailed his interior EOS, it is not possible to pursue this point further. Note, however, that the treatment of crystallization in Hansen's calculations has been demonstrated to be incorrect (Isern et al. 2000). We thus disagree with him about the importance of chemical fractionation at crystallization, as discussed in the next subsection. Note also that apparently Hansen's calculations do not extend beyond log $(L/L_\odot) \sim -5.0$, which corresponds to an age of $t \sim 12$ Gyr for a 0.6 $M_\odot$ WD.

3.1.2. *Effects of Internal Composition and Crystallization*

Figure 3 illustrates also the effect of initial C/O stratification on the cooling time for a 0.6 $M_\odot$ H atmosphere WD, as examined in detail by Salaris et al. (1997). The rightmost dot-dashed curve displays the cooling sequence of our reference model with an initial C/O profile resulting from a low (CF88) $^{12}C(\alpha, \gamma)^{16}O$ reaction rate, to be compared with the sequence obtained with a high-rate (Caughlan et al. 1985) induced profile (*rightmost solid line*). A larger rate yields a larger initial oxygen-enriched core and affects the cooling in several ways (Segretain et al. 1994; Salaris et al. 1997): (1) the larger oxygen content corresponds to a smaller heat capacity $[C_V \propto \sum_i (X_i/A_i)]$ and thus to a faster cooling prior to crystallization, (2) the gravitational energy release at crystallization, $\Delta E \propto (\Delta\rho/\rho)Mg$, is smaller because of the spindle form of the phase diagram (Segretain & Chabrier 1993; Segretain et al. 1994; Chabrier 1997), but (3) the total amount of oxygen to be differentiated is larger (cf. effect [1]), and (4) crystallization occurs earlier in the evolution since oxygen crystallizes at a higher temperature than carbon. Whether this corresponds to a larger *effective* temperature depends on the L-T_c (and thus $T_{\rm eff}$-T_c) relation for each WD mass (Fig. 2). As shown by Salaris et al. (1997), effects (2)–(4) more or less compensate for both reaction rate–induced profiles, and the time delay induced by crystallization $\Delta\tau = \Delta E/L$ is about the same for these two stratified profiles. The difference in cooling times thus stems primarily from the available heat content (effect [1]). For example, at a luminosity log $(L/L_\odot) = -4.5$ (resp. -5.0), our reference 0.6 $M_\odot$ model has an age of $t = 10.3$ (resp. 12.7) Gyr whereas the same luminosity corresponds to an age $t = 10.7$ (resp. 13.3) Gyr for a low-rate initial profile (see Fig. 3), confirming the Salaris et al. (1997) analysis. This illustrates the present uncertainty in cooling times due to uncertainties in the $^{12}C(\alpha, \gamma)^{16}O$ reaction rate and induced WD initial internal composition.

Another uncertainty affecting the internal composition is the exact shape of the C/O crystallization diagram. In the present calculations, we use the Segretain & Chabrier (1993) spindle diagram, calculated within the framework of the density-functional theory of freezing. The Barrat, Hansen, & Mochkovitch (1988) calculations were based on previous (obsolete) values of the plasma parameter Γ at crystallization but would yield similar results if updated (see Segretain & Chabrier 1993), whereas the Ichimaru, Iyetomi, & Ogata (1988) azeotropic C/O diagram is demonstrably erroneous (DeWitt, Slattery, & Chabrier 1996). Figures 3 and 4 illustrate the effect of chemical fractionation at crystallization, resulting from the difference of abundance of carbon and oxygen in the fluid and in the solid phase, on a 0.6 $M_\odot$ WD. This induces a variation of chemical potential at constant volume and temperature (Chabrier 1997) that provides an additional source of energy (Mochkovitch 1983; García-Berro et al. 1988; Segretain et al. 1994). Although this energy amounts to only $\sim$1% of the binding energy of the star, it is released at a low luminosity and thus lengthens appreciably the lifetime of the star (Chabrier 1997; Isern et al. 1997). For example, a luminosity log $(L/L_\odot) = -4.5$ (resp. -5.0) for our stratified profile corresponds to an age $t = 8.8$ (resp. 11.4) Gyr if fractionation is ignored and $t = 10.3$ (resp. 12.7) Gyr if it is taken into account. As seen in Figure 3, once crystallization has proceeded throughout the entire star, the time delay remains constant and amounts to from $\sim$1 Gyr for the least (0.5 $M_\odot$) and most (1.2 $M_\odot$) massive WDs to a maximum value of about 1.5 Gyr for our reference 0.6–0.8 $M_\odot$ WDs. The effect thus remains substantial and must be properly taken into account in WD cooling theory. This is at odds with Hansen's (1999) results, as explained in § 3.1.1. As seen in Figure 3, crystallization in our calculations occurs at a later age and a fainter luminosity than in the Wood (1995) or Montgomery et al. (1999) calculations. This reflects the

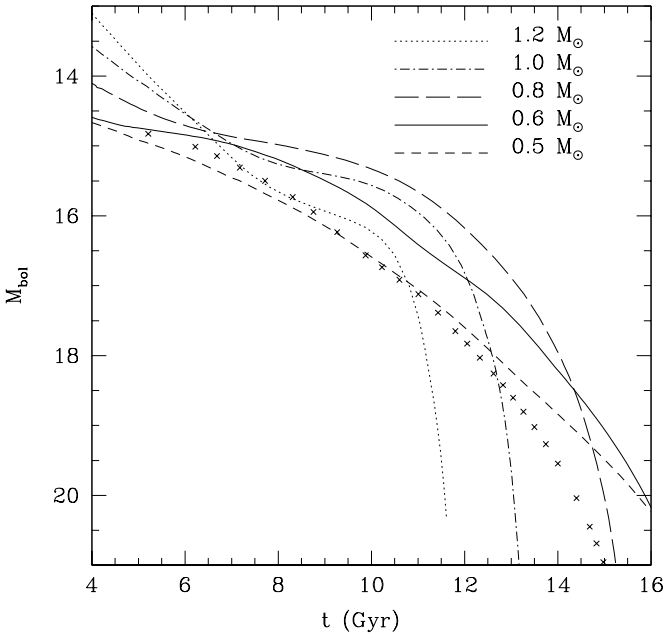


FIG. 4.—Cooling sequences $M_{bol}(t)$ for different masses for our reference model DA WDs. The crosses indicate the cooling sequence for a 0.6 $M_\odot$ WD if the energy release due to C/O chemical fractionation at crystallization is not included in the cooling (see text).

faster cooling for Wood's and Montgomery's calculations, as discussed in § 3.1.1. This translates into a smaller crystallization-induced delay in the latter case since $\Delta\tau \propto 1/L$.

Although the crystallization model for binary ionic mixtures has not yet been verified observationally in WDs, it has been studied for a long time by geophysicists (see, e.g., Loper 1984; Buffett et al. 1992). Although the nature of the plasma (or alloy) is different, the *physics* of the process (thermodynamics and energy transport) is exactly the same. Note, however, that these crystallization-induced delays represent upper limits. Indeed, the present calculations assume complete mixing of the C-enriched fluid layers, i.e., a maximum efficiency for this process. This is supported by the fact that the mixing instability timescale is much shorter than the evolutionary timescale (Mochkovitch 1983). Figure 4 displays the cooling sequences $M_{bol}(t)$ for different masses for our reference model calculations.

3.2. *Cooling Times*

Figure 5 displays the mass-T_{eff} relation, or equivalently the radius- or surface gravity–T_{eff} relation (see Tables 1–5), for several constant WD cooling times. Before crystallization sets in, massive WDs evolve more slowly because of their greater energy content (C_V) and their smaller radiative surface areas.[4] Since they are hotter and brighter at a given T_c than less massive WDs, and since crystallization occurs always at the same internal temperature T_c, massive WDs crystallize earlier and at a higher T_{eff} and L. At this stage, the crystallized core enters the Debye cooling regime ($C_V \propto T^3$) and cools more quickly. This crystallization process causes the bending on the cooling times to be downward.

Figure 6 displays the same constant cooling times as a function of absolute M_V magnitude. The bulk of all H atmosphere WDs, those with $m \lesssim 0.8\ M_\odot$ (assuming a WD

[4] Remember the objects under consideration are cool enough so that the neutrino luminosity is completely negligible.

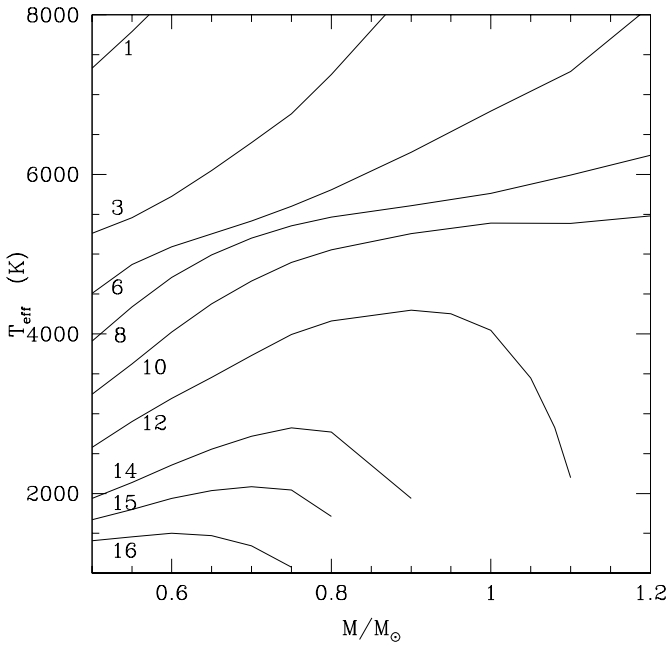


FIG. 5.—Mass-T_{eff} constant cooling times for H atmosphere WDs. Ages are indicated in Gyr for each curve.

TABLE 1

COOLING SEQUENCE FOR A 0.5 $M_\odot$ WHITE DWARF OF OUR REFERENCE MODEL

Age	T_{eff}	log g	M_{bol}	M_B	M_V	M_R	M_I	M_J	M_H	M_K
1	7333	7.837	12.96	13.53	13.17	12.94	12.67	12.48	12.33	12.33
3	5263	7.863	14.45	15.41	14.70	14.25	13.79	13.28	13.01	12.92
6	4509	7.872	15.15	16.37	15.48	14.92	14.36	13.78	13.64	13.63
8	3911	7.874	15.78	17.16	16.12	15.47	14.82	14.31	14.33	14.40
10.....	3243	7.875	16.59	17.89	16.72	16.00	15.40	15.46	15.67	15.90
12.....	2578	7.877	17.59	18.65	17.33	16.68	16.54	17.10	17.27	17.79
13.....	2233	7.877	18.22	19.12	17.70	17.15	17.51	18.18	18.23	19.10
14.....	1938	7.877	18.83	19.61	18.10	17.66	18.63	19.34	19.23	20.58
15.....	1670	7.877	19.48	20.16	19.94	18.25	19.94	20.67	20.34	22.31

NOTE.—The age is in Gyr, T_{eff} is in K, the surface gravity $g = GM/R^2$ in cgs. $M_{bol} = -2.5 \log (L/L_\odot) + 4.75$. The VRI magnitudes are in the Johnson-Cousins system (Bessell 1990), JHK in the CIT system (Leggett 1992). Absolute calibration from the observed spectrum of Vega (Mountain et al. 1985).

TABLE 2

COOLING SEQUENCE FOR A 0.6 $M_\odot$ WHITE DWARF

Age	$T_{\rm eff}$	log g	$M_{\rm bol}$	M_B	M_V	M_R	M_I	M_J	M_H	M_K
1	8273	8.001	12.67	13.24	12.95	12.76	12.56	12.49	12.38	12.41
3	5726	8.023	14.31	15.11	14.50	14.11	13.71	13.28	13.03	12.96
6	5091	8.032	14.84	15.85	15.10	14.62	14.14	13.60	13.36	13.30
8	4709	8.035	15.19	16.34	15.50	14.97	14.44	13.87	13.70	13.68
10.....	4024	8.038	15.88	17.22	16.22	15.58	14.95	14.40	14.40	14.46
12.....	3190	8.039	16.88	18.14	16.96	16.25	15.68	15.84	16.06	16.32
13.....	2813	8.039	17.44	18.57	17.31	16.62	16.27	16.73	16.93	17.34
14.....	2355	8.040	18.21	19.14	17.76	17.18	17.38	18.02	18.11	18.85
15.....	1938	8.040	19.05	19.80	18.30	17.88	18.87	19.58	19.47	20.81

mass distribution similar to the one observed in the disk), remains brighter than $M_V \simeq 18$ after 14 Gyr.

3.3. *Color-Magnitude and Color-Color Diagrams*

Figures 7 and 8 display cooling sequences in M_V-versus-$(V-I)$ and M_J-versus-$(J-K)$ diagrams, respectively. WDs with a small admixture of helium in the atmosphere will have similar colors (see Tables 1 and 2 of BSW95). The triangles illustrate the coolest disk WDs identified spectroscopically as H-rich atmosphere WDs by Leggett, Ruiz, & Bergeron (1998). Collision-induced absorption by H_2 at $T_{\rm eff} \sim 4500$–5000 K causes the turnover to bluer $J-K$ at $M_J \sim 13$–15, depending on the mass. At these temperatures, the effect is still modest and a large fraction of the flux emerges longward of 1 μm (see Fig. 5 of BSW95). As $T_{\rm eff}$ decreases, however, the CIA becomes stronger, causing a turnover in the optical colors near $M_V \sim 16$–17 at later stages of the evolution. The 12 Gyr curve forms a loop in the M_V-versus-$(V-I)$ diagram. This stems from the very different cooling rates of WDs for different masses. As mentioned above, less massive WDs cool faster initially because

TABLE 3

COOLING SEQUENCE FOR A 0.8 $M_\odot$ WHITE DWARF

Age	$T_{\rm eff}$	log g	$M_{\rm bol}$	M_B	M_V	M_R	M_I	M_J	M_H	M_K
1	10394	8.316	12.14	12.79	12.57	12.49	12.44	12.53	12.51	12.58
3	7253	8.325	13.73	14.30	13.94	13.69	13.41	13.22	13.06	13.06
6	5806	8.331	14.71	15.49	14.89	14.50	14.12	13.71	13.48	13.41
8	5464	8.335	14.98	15.85	15.19	14.77	14.35	13.88	13.64	13.57
10.....	5053	8.337	15.33	16.33	15.58	15.10	14.62	14.09	13.88	13.84
12.....	4162	8.340	16.18	17.42	16.47	15.86	15.26	14.76	14.77	14.83
13.....	3538	8.340	16.88	18.16	17.07	16.39	15.76	16.65	15.83	16.00
14.....	2768	8.341	17.95	19.02	17.77	17.10	16.82	17.31	17.51	17.93
15.....	1713	8.34 1	20.02	20.68	19.11	18.80	20.37	21.10	20.80	22.64

TABLE 4

COOLING SEQUENCE FOR A 1.0 $M_\odot$ WHITE DWARF

Age	$T_{\rm eff}$	log g	$M_{\rm bol}$	M_B	M_V	M_R	M_I	M_J	M_H	M_K
1	13680	8.621	11.47	12.55	12.43	12.48	12.53	12.75	12.77	12.84
3	9609	8.629	13.02	13.66	13.41	13.27	13.16	13.21	13.16	13.22
6	6794	8.633	14.54	15.15	14.72	14.43	14.13	13.89	13.70	13.68
8	5761	8.636	15.26	16.04	15.43	15.04	14.66	14.24	14.02	13.95
10.....	5389	8.639	15.56	16.45	15.77	15.33	14.91	14.44	14.21	14.14
12.....	4045	8.64 0	16.81	18.03	17.06	16.45	15.85	15.45	15.51	15.61
13.....	2107	8.641	19.64	20.43	19.01	18.53	19.18	19.85	19.84	20.88

TABLE 5

COOLING SEQUENCE FOR A 1.2 $M_\odot$ WHITE DWARF

Age	$T_{\rm eff}$	log g	$M_{\rm bol}$	M_B	M_V	M_R	M_I	M_J	M_H	M_K
1	21950	8.995	10.15	12.27	12.34	12.45	12.58	13.02	13.09	13.10
3	13534	9.004	12.27	13.34	13.20	13.26	13.31	13.52	13.54	13.61
6	8105	9.009	14.51	15.11	14.80	14.57	14.36	14.29	14.17	14.19
8	6242	9.011	15.65	16.33	15.81	15.47	15.13	14.80	14.60	14.55
10.....	5479	9.013	16.22	17.08	16.42	16.00	15.58	15.12	14.91	14.85

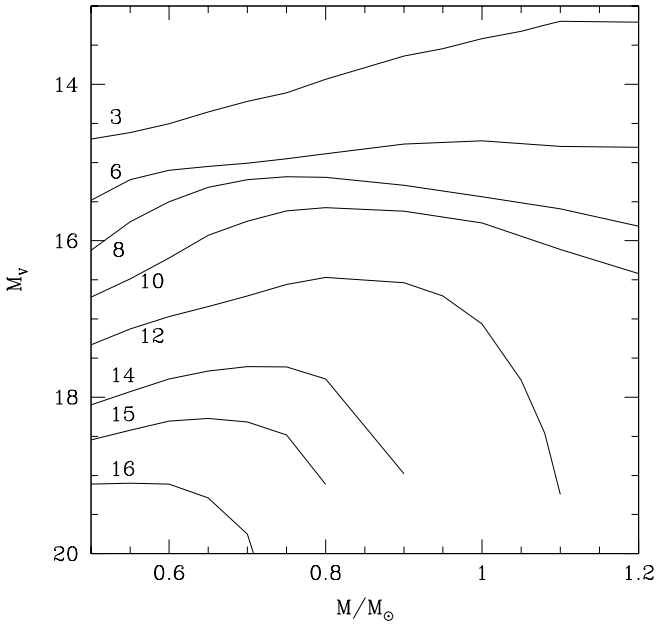


FIG. 6.—Mass-M_V constant cooling times for H atmosphere WDs

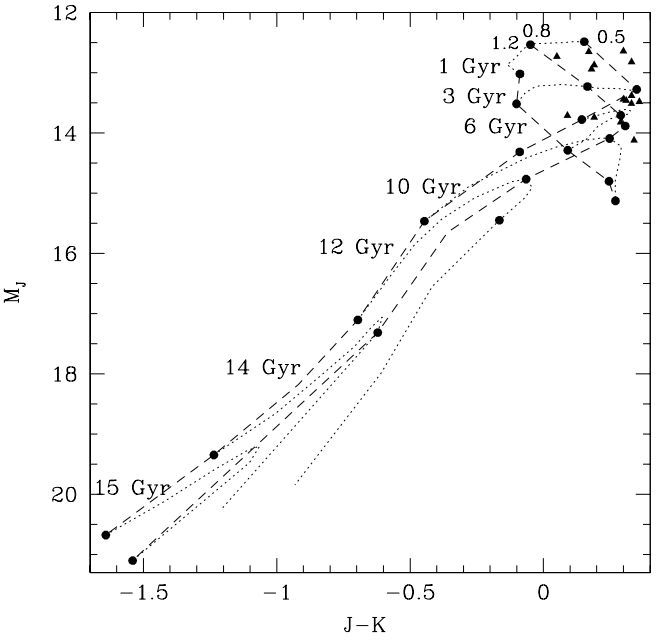


FIG. 8.—Same as Fig. 6, but for an M_J vs. $(J-K)$ color-magnitude diagram.

of their smaller heat content, whereas massive WDs crystallize earlier and then enter the rapid Debye cooling regime. The combination of these two effects yields the slowest cooling rate for $\sim 0.8\ M_\odot$ WDs after ~ 8 Gyr, whereas both the least and most massive objects cool faster, reaching fainter magnitudes and bluer colors at younger ages.

Figure 9 shows a color-color diagram comparing optical and near-IR colors for a 0.6 and a 1.2 $M_\odot$ H atmosphere WD. Note that gravity does not affect the qualitative behavior of the diagram. Indeed, increasing gravity has an effect similar to decreasing the effective temperature on the spectrum (see, e.g., Saumon et al. 1994). Naturally the age dependence is different, as shown on the figure by the solid circles and squares, respectively. As already mentioned in Chabrier (1999), we note from the previous figures the strong dependence of colors upon age for $t \gtrsim 12$ Gyr. If the gravity, i.e., the mass of such a WD, can be determined independently, this provides a powerful tool to determine the age of the Galactic halo.

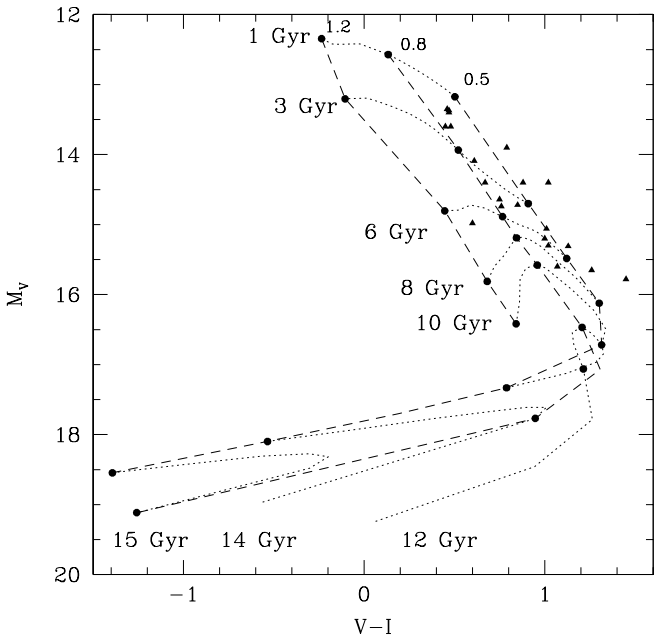


FIG. 7.—M_V vs. $(V-I)$ color-magnitude diagram for pure H atmosphere WDs. Constant WD cooling times correspond to the dotted lines. Cooling sequences for 0.5, 0.8, and 1.2 $M_\odot$ are indicated by the dashed lines. The triangles correspond to the Leggett et al. (1998) WDs identified as H-rich atmosphere WDs.

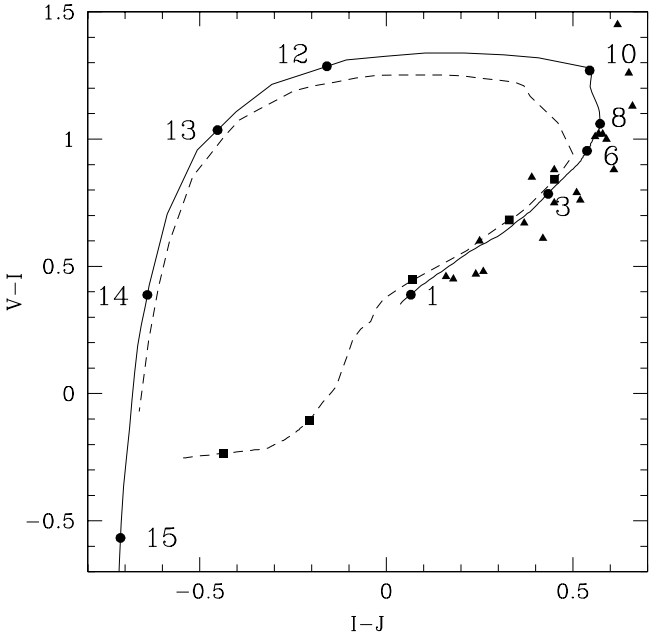


FIG. 9.—Color-color $(V-I)$-$(I-J)$ diagram for a 0.6 $M_\odot$ (*solid line*) and a 1.2 $M_\odot$ WD (*dashed line*). Cooling times are indicated in Gyr and are labeled for the 0.6 $M_\odot$ WD (*solid dots*). The squares correspond to the same ages for the 1.2 $M_\odot$ WD. For this mass the end of the track corresponds to 11.6 Gyr. The triangles correspond to the Leggett et al. (1998) WDs identified as H-rich atmosphere WDs.

Tables 1–5 give the characteristic properties of the present WD H atmosphere cooling sequences in various broadband filters for the mass-range characteristic of WDs with C/O cores.

4. CONCLUSION

We have computed evolutionary sequences for cool ($T_{\rm eff} < 10{,}000$ K) pure H atmosphere WDs, although the calculations can be applied to WDs with a small admixture of He in the atmosphere as well, using appropriate color indices (BSW95). These models are primarily aimed at identifying old, cool WDs in the Galactic old disk, in the spheroid or dark halo, or in globular clusters once fainter detection limits can be achieved. We have first improved upon the EOS of the fully ionized interior to calculate accurate cooling sequences for crystallized WDs, namely, objects fainter than $\log (L/L_\odot) \sim -4.5$ ($t \gtrsim 10$ Gyr for 0.6 $M_\odot$). These WDs are in a quantum regime. The temperature-dependent contributions, in particular the ion-electron energy of a quantum, relativistic ion-electron plasma, are the only sources of specific heat and thus determine entirely the thermal reservoir to be radiated into space, even though they provide a negligible contribution to the internal energy. We have next obtained improved L-T_c relations that govern the rate of cooling of white dwarfs. The envelope and atmosphere calculations include state-of-the-art radiative opacities down to $T_{\rm eff} = 1500$ K for pure hydrogen. We have examined and quantified the uncertainties in these cooling sequences arising from (1) the initial C/O stratification of the WD, which follows from the $^{12}{\rm C}(\alpha, \gamma)^{16}{\rm O}$ reaction rate; (2) the L-T_c relation (the core-surface boundary condition); and (3) the crystallization-induced gravitational energy release. The uncertainty in the $^{12}{\rm C}(\alpha, \gamma)^{16}{\rm O}$ reaction rate translates into a $\lesssim 0.5$ Gyr difference in cooling time. The uncertainty due to different L-T_c relations when using accurate boundary conditions yields substantial differences in the range $(L/L_\odot) \sim 10^{-4.0}$ to $10^{-4.5}$, when, for the first time, the superficial convection zone reaches the degenerate core. This is probably due to the detailed physics entering the core (EOS) and envelope (EOS, $\nabla_{\rm rad}$, $\nabla_{\rm cond}$) calculations. These differences, however, vanish almost entirely below this limit, i.e., for $t \gtrsim 10$ Gyr. The maximum time delay induced by chemical fractionation at crystallization amounts to $\sim$1–1.5 Gyr, depending on the WD mass, and represents one of the major uncertainties in dating very cool WDs from their observed luminosity. Future laser-driven experiments on the crystallization of dense plasmas should shed light on this complicated physics problem, which bears major consequences in the present astrophysical context. The other major uncertainty in WD cooling stems from the ill-determined mass fraction of hydrogen and helium in the external envelope, in particular for old WDs originating from metal-depleted progenitors.

We find noticeable differences ($\gtrsim 1$ Gyr) between our and Hansen's (1999) cooling sequences. Part of it very likely stems from the different treatments of the interior EOS and envelope EOS and opacities, but also from the demonstrably underestimated crystallization-induced time delay in Hansen's calculations. An $\sim$0.5–1 mag difference in colors occurs also for $V-I \lesssim 1$ between Hansen's and our calculations, which most likely arises from details of the calculation of the atmosphere models, including the nonideal effects (see Fig. 3 of SJ99). This shows that, although a consistent general theory for the cooling of cool WDs is emerging, work remains to be done to reach more robust results. The theory is still very uncertain for very cool helium-rich atmosphere WDs. A correct calculation of helium pressure ionization and of the He^- free-free absorption cross section at high densities in the atmosphere of these objects remains to be done. Attention must also be devoted to dense atmospheres including a trace of metals since the subsequent increase in opacity will affect dramatically the cooling of the star. Work in this direction is in progress.

Meanwhile, the present calculations should provide what we believe to be presently the most accurate calculations of very cool white dwarf sequences. They provide a useful basis to search for and to identify faint, old WDs either in the field or in globular clusters. By allowing the determination of the mass and age of possible halo WDs (Hodgkin et al. 2000; Ibata et al. 2000), they will also provide important constraints on the age of the Galactic disk and halo and on the Galaxy initial mass function.[5]

We thank M. A. Wood and B. Hansen for kindly providing models and results from their calculations, M. Hernanz for providing tables of the stratified profiles, and A. Potekhin for stimulating discussions. This work was supported in part by NSF grant AST 97-31438 to D. S.

[5] The present models in various filters are available upon request from Gilles Chabrier (chabrier@ens-lyon.fr).

REFERENCES

Adams, F., & Laughlin, G. 1996, ApJ, 468, 58
Arnould, M., et al. 1999, Nucl. Phys. A, 656, 3
Bahcall, J., Flynn, C., Gould, A., & Kirhakos, S. 1994, ApJ, 435, L51
Barrat, J. L., Hansen, J. P., & Mochkovitch, R. 1988, A&A, 199, L15
Bergeron, P., Ruiz, M.-T., & Leggett, S. K. 1997, ApJS, 108, 339
Bergeron, P., Saumon, D., & Wesemael, F. 1995a, ApJ, 443, 764 (BSW95)
Bergeron, P., Wesemael, F., & Beauchamp, A. 1995b, PASP, 107, 1047 (BWB95)
Bergeron, P., Wesemael, F., & Fontaine, G. 1991, ApJ, 367, 253
Bessell, M. S. 1990, PASP, 102, 1181
Blöcker, T., Herwig, F., Driebe, T., Bramkamp, H., & Schönberner, D. 1997, in Proc. 10th European Workshop on White Dwarfs, White Dwarfs, ed. J. Isern, M. Hernanz, & E. García-Berro (Dordrecht: Kluwer), 57
Böhm, K.-H., Carson, T. R., Fontaine, G., & Van Horn, H. M. 1977, ApJ, 217, 521
Brassard, P., & Fontaine, G. 1994, in IAU Colloq. 147, The Equation of State in Astrophysics, ed. G. Chabrier & E. Schatzman (Cambridge: Cambridge Univ. Press), 560
———. 1997, in Proc. 10th European Workshop on White Dwarfs, White Dwarfs, ed. J. Isern, M. Hernanz, & E. García-Berro (Dordrecht: Kluwer), 451
Buffett, B. A., Huppert, H. E., Lister, J. R., & Woods, A. W. 1992, Nature, 356, 329
Caughlan, G. R., & Fowler, W. A. 1988, At. Data Nucl. Data Tables, 36, 411 (CF88)
Caughlan, G. R., Fowler, W. A., Harris, M. J., & Zimmermann, B. A. 1985, At. Data Nucl. Data Tables, 32, 197
Chabrier, G. 1997, in IAU Symp. 189, Fundamental Stellar Properties, ed. T.R. Bedding et al. (Dordrecht: Kluwer), 381
———. 1999, ApJ, 513, 103
Chabrier, G., Segretain, L., & Méra, D. 1996, ApJ, 468, L21

D'Antona, F., & Mazzitelli, I. 1990, ARA&A, 28, 139
DeWitt, H., Slattery, W., & Chabrier, G. 1996, Phys. Lett. A, 228, 21
Fontaine, G., Graboske, A., & Van Horn, H. M. 1977, ApJS, 35, 293
Fontaine, G., & Van Horn, H. M. 1976, ApJS, 31, 467
Fontaine, G., & Wesemael, F. 1997, in Proc. 10th European Workshop on White Dwarfs, White Dwarfs, ed. J. Isern, M. Hernanz, & E. García-Berro (Dordrecht: Kluwer), 173
García-Berro, E., Hernanz, M., Isern, J., & Mochkovitch, R. 1988, A&A, 193, 141
Graff, D., Laughlin, G., & Freese, L. 1998, ApJ, 499, 7
Hansen, B. M. S. 1998, Nature, 394, 860
———. 1999, ApJ, 520, 680
Harris, H. C., Dahn, C. C., Vrba, F. J., Henden, A. A., Liebert, J., Schmidt, G. D., & Reid, I. N. 1999, ApJ, 524, 1000
Hodgkin, S., Oppenheimer, B., Hambly, N., Jameson, R., Smartt, S., & Steele, I. 2000, Nature, 403, L57
Hubbard, W. B., & Lampe, M. 1969, ApJS, 18, 297
Ibata, R., Irwin, M., Bienaymé, O., Scholz, R., & Guibert, J. 2000, ApJ, 532, L41
Ibata, R., Richer, H., Gilliland, R., & Scott, D. 1999, ApJ, 524, L95
Ichimaru, S., Iyetomi, H., & Ogata, S. 1988, ApJ, 334, L17
Iglesias, C. A., & Rogers, F. J. 1996, ApJ, 464, 943
Isern, J., García-Berro, E., Hernanz, M., & Chabrier, G. 2000, ApJ, 528, 397
Isern, J., Hernanz, M., Mochkovitch, R., & García-Berro, E. 1991, A&A, 241, L29
Isern, J., Mochkovitch, R., Hernanz, M., & García-Berro, E. 1997, ApJ, 485, 308
Itoh, N., Hatashi, H., & Kohyama, Y. 1993, ApJ, 418, 405
Itoh, N., Mitake, S., Iyetomi, H., & Ichimaru, S. 1983, ApJ, 273, 774
Koester, D., & Chanmugam, G. 1990, Rep. Prog. Phys., 53, 837
Lamb, D. Q., & Van Horn, H. M. 1975, ApJ, 200, 306
Leggett, S. K. 1992, ApJS, 82, 351
Leggett, S. K., Ruiz, M.-T., & Bergeron, P. 1998, ApJ, 497, 294
Lenzuni, P., Chernoff, D. F., & Salpeter, E. E. 1991, ApJS, 76, 759
Loper, D. E. 1984, Adv. Geophys., 26, 1
Méndez, R., & Minniti, D. 2000, ApJ, 529, 911
Méndez, R., Minniti, D., de Marchi, G., Baker, A., & Couch, W. 1996, MNRAS, 283, 666
Mestel, L., & Ruderman, M. A. 1967, MNRAS, 136, 27
Mochkovitch, R. 1983, A&A, 122, 212
Montgomery, M. H., Klumpe, E., Winget, D. E., & Wood, M. 1999, ApJ, 525, 482
Mountain, C. M., Selby, M. J., Leggett, S. K., Blackwell, D. E., & Petford, A. D. 1985, A&A, 151, 399
Nelson, R., Santiago, B., & Gilmore, G. 1996, NewA, 1, 1
Potekhin, A. Y., Baiko, D. A., Haensel, P., & Yakovlev, D. 1999, A&A, 346, 345
Potekhin, A. Y., & Chabrier, G. 2000, Phys. Rev. E, in press
Rogers, F., & Iglesias, C. 1992, ApJS, 79, 507
Salaris, M., Dominguez, I., García-Berro, E., Hernanz, M., Isern, J., & Mochkovitch, R. 1997, ApJ, 486, 413
Salpeter, E. E. 1961, ApJ, 134, 669
Saumon, D., Bergeron, P., Lunine, J. I., Hubbard, W. B., & Burrows, A. 1994, ApJ, 424, 333
Saumon, D., Chabrier, G., & Van Horn, H. M. 1995, ApJS, 99, 713 (SCV95)
Saumon, D., & Jacobson, S. B. 1999, ApJ, 511, L107 (SJ99)
Segretain, L. 1996, A&A, 310, 485
Segretain, L., & Chabrier, G. 1993, A&A, 271, L13
Segretain, L., Chabrier, G., Hernanz, M., García-Berro, E., Isern, J., & Mochkovitch, R. 1994, ApJ, 429, 641
Tassoul, M., Fontaine, G., & Winget, D. E. 1990, ApJS, 72, 335
Wood, M. A. 1992, ApJ, 386, 536
———. 1995, in White Dwarfs, ed. D. Koester & K. Werner (Berlin: Springer), 105
Wood, M. A., & Winget, D. E. 1989, in IAU Colloq. 114, White Dwarfs, ed. G. Wegner (Berlin: Springer), 282
Yakovlev, D., & Shalybkov, D. 1989, Astron. Space Phys. Rev., 7, 311 (YS89)